Impact of earthquakes vs. heat waves on the socioeconomic losses of buildings

Bianchi, S.; Ciurlanti, J.; Navarro, A. Luna; Brembilla, E.

DOI
10.7712/120123.10752.21303

Publication date
2023

Document Version
Final published version

Published in
COMPDYN Proceedings

Available online at www.eccomasproceedia.org
Eccomas Proceedia COMPDYN (2023) 4706-4718

ECCOMAS
Proceedia

COMPDYN 2023
9th ECCOMAS Thematic Conference on
Computational Methods in Structural Dynamics and Earthquake Engineering
M. Papadrakakis, M. Fragiadakis (eds.)
Athens, Greece, 12-14 June 2023

IMPACT OF EARTHQUAKES VS. HEAT WAVES ON THE SOCIO-ECONOMIC LOSSES OF BUILDINGS

S. Bianchi[1], J. Ciurlanti[2], A. Luna Navarro[1], and E. Brembilla[1]

[1] Delft University of Technology
Julianalaan 134, Delft 2628 BL, Netherlands
{s.bianchi, a.lunanavarro, e.brembilla}@tudelft.nl

[2] Arup
Naritaweg 118, Amsterdam 1043 CA, Netherlands
jonathan.ciurlanti@arup.com

Abstract

Recent earthquakes have confirmed the vulnerability of our built environment, resulting in significant socio-economic losses, market disruptions, and environmental damage. Additionally, climate change is causing more frequent and severe weather-related events such as heat waves, which are impacting the construction sector and the health and well-being of building occupants. This emphasizes the pressing need to increase society's overall resilience by focusing on the various hazards that buildings may encounter throughout their lifespan. Although the need for a multi-risk analysis has been recognized in current performance-based design approaches, existing studies mostly focus on single hazards thereby neglecting the impact assessment of multiple hazards on the building performance.

This paper explores the economic and social losses of buildings due to earthquakes and heat waves. The study focuses on a high-rise building consisting of a reinforced concrete structure and masonry/cladding facades, and designed for two different locations in Europe. By means of a numerical model, time-history non-linear analyses are carried out to estimate the probable maximum losses in terms of repair costs and injuries/fatalities. In addition to earthquake scenarios, the study conducts dynamic energy simulations and comfort analyses that consider local climate scenarios and extreme heat events. The energy analysis calculates the economic losses caused by weather-related power consumption while the impact on occupants is assessed in terms of discomfort hours. Results from the seismic and energy simulations are finally compared to quantify and discuss the impact of the two different extreme hazards on the building performance and their potential consequences.

Keywords: Earthquakes, Heat waves, Building performance, Socio-economic losses.

doi: 10.7712/120123.10752.21303

1 INTRODUCTION

The vulnerability of our existing building stock to natural disasters such as earthquakes was once again highlighted by recent tragic events, such as the devastating Turkey and Syria earthquake of 2023 (Figure 1a). Such disasters can result in severe direct and indirect economic losses and casualties. Direct losses include damage to buildings, loss of life, and injury, while indirect losses include reduced productivity and loss of income. Climate-related extreme events, such as more severe and frequent heat waves, are also increasingly impacting both the economy and society. In urban areas, buildings and infrastructure are often ill-equipped to cope with high temperatures, leading to significant socio-economic losses. The impact of heat waves on buildings can include increased energy consumption for cooling, reduced indoor air quality, and structural damage. When considering the overall impact of multiple hazards such as geophysical events (including earthquakes) and climatological events like heat waves, the total losses can be substantial, as shown in Figure 1b. According to recent data [1], heat waves have been responsible for the majority of fatalities in the last few decades, accounting for 68% of the total. Meanwhile, earthquakes have caused the greatest economic losses, representing 22% of the total value. Interestingly, despite their devastating impacts, both of these events have resulted in relatively low insurance losses, in contrast to meteorological events such as storms, which account for 62% of total insurance losses.

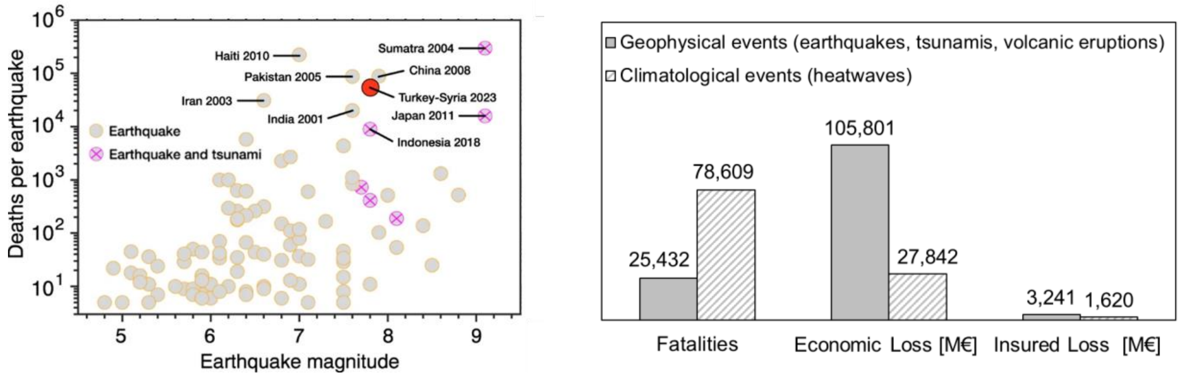

(a) (b)

Figure 1: (a) Impact of Turkey and Syria earthquakes: the fifth worst earthquake since 2000 [2]. (b) Social and economic losses for the period 1980-2017 (data elaborated from the European Environment Agency [1]).

Therefore, it is crucial to consider the potential impact of these hazards throughout the lifespan of buildings and take appropriate measures in design and retrofitting choices to enhance their resilience. This would not only help to minimize socio-economic losses and casualties, but also contribute to creating a safer and more sustainable built environment.

Focusing on earthquakes, different approaches have been developed for vulnerability assessments and loss estimation. In addition to empirical models that estimate damage and losses based on building characteristics such as age, height, and construction type [3, 4], the Performance-Based Earthquake Engineering (PBEE) methodology provides a probabilistic component-based approach to loss modeling [5-7]. PBEE enables the direct evaluation of performance measures such as economic losses, downtime, and casualties that are relevant to stakeholders for managing decisions related to investments and seismic risk mitigation. This comprehensive framework includes the description, definition, and qualification of different variables while considering all inherent uncertainties in earthquake performance assessment. Numerous loss assessment investigations can be found in the literature, focusing on both scenario or intensity-based analyses as well as time-based assessments [e.g. 8-9]. Overall, most of these studies have focused on assessing the direct and indirect losses resulting from earthquakes on buildings, rather than potential fatalities. The findings emphasize the importance of implementing measures to improve building resilience to earthquakes, and the need for effective policies and strategies to mitigate the impact of earthquakes on buildings, such the adoption of a damage-control philosophy and technologies [10].

When assessing the impacts of heat waves on buildings, energy building performance simulation models [11] and/or empirical data collection through environmental and comfort monitoring [e.g. 12] are typically developed to estimate energy consumption and user response under varying environmental conditions. Several studies have used building performance simulation models to estimate economic losses resulting from increased power consumption [13], as well as the impact on the indoor thermal environment. Conversely, the estimation of potential fatalities caused by high internal temperatures is poorly addressed due to the lack of empirical data available on individual occupant response in buildings during heat waves [14], and this is a barrier to effectively estimate the social losses associated with heat waves depending on building design. Previous research has focused on the relationship between outdoor condition and mortality rate [e.g. 15], while only two studies at the best of our knowledge have studied the relationship between indoor temperature, building characteristics and related mortality rate during heat waves [16].

Although methods are further developing and research efforts are growing on the two separate domains (earthquakes and heat waves), an assessment of the potential losses due to the two hazards is still missing. This paper presents an integrated analysis of the overall impacts resulting from earthquakes and heat waves based on the local scenario. The aim is to compare the direct economic and social losses associated with these events and to highlight the need for integrated assessment to facilitate more effective investment decisions for building projects.

2 RESEARCH METHODOLOGY

This paper investigates the direct losses (potential casualties, economic losses) of buildings due to earthquakes compared to heat waves, focusing on a reinforced concrete high-rise new building with precast concrete façade systems as a case study. The selection of this case study is based on the significant impact that high-rise buildings can have on society, urban planning, and the economy of modern cities, especially during extreme events due to the larger number of occupants.

Seismic and energy modelling and simulations are carried out for the high-rise building designed for two different locations. Specifically, non-linear time history analysis and dynamic energy simulations are implemented to assess the seismic and energy performance of the building, respectively. The seismic loss modelling is implemented by following the above-mentioned probabilistic-based PEER procedure, that enables to assess the expected damage due earthquake scenarios to both structural and non-structural components thus assessing the consequent losses. The economic losses due to the heat wave are instead estimated by computing the total energy cost due to higher cooling and ventilation demand during the heat wave. For the social losses, no model can be found in literature that correlate indoor air temperature to mortality rate during heatwaves. Therefore, the cumulative hours of overheating are calculated by considering the indoor operative temperature at the center of the thermal zone and the following comfort thresholds: 26 °C, 28 °C, 30 °C and 32 °C. Temperature above 28 °C are considered to be a hazard for human health, while temperature above 32 °C are considered an extreme hazard for human health.

The simulation results provide a quantification of the impact associated with earthquakes and weather-related extreme events in terms of building performance and potential consequences. An integrated multi-hazard analysis is therefore suggested for informing more effective decision-making from the early-stage design process, thus targeting an acceptable level of overall resilience.

3 APPLICATION TO A CASE STUDY

3.1 Description of the case study

The case study is a 18-storey reinforced concrete tower with regularity in plan and elevation. The building scheme derives from a previous study developed by the authors [17]. The tower has plan dimension of 22.05m (spans of 7.35m) in both structural directions and an inter-story height of 3m (Figure 2). The building has open-plan office floors at leach level apart from the last three levels that are residential, while the building roof is not accessible.

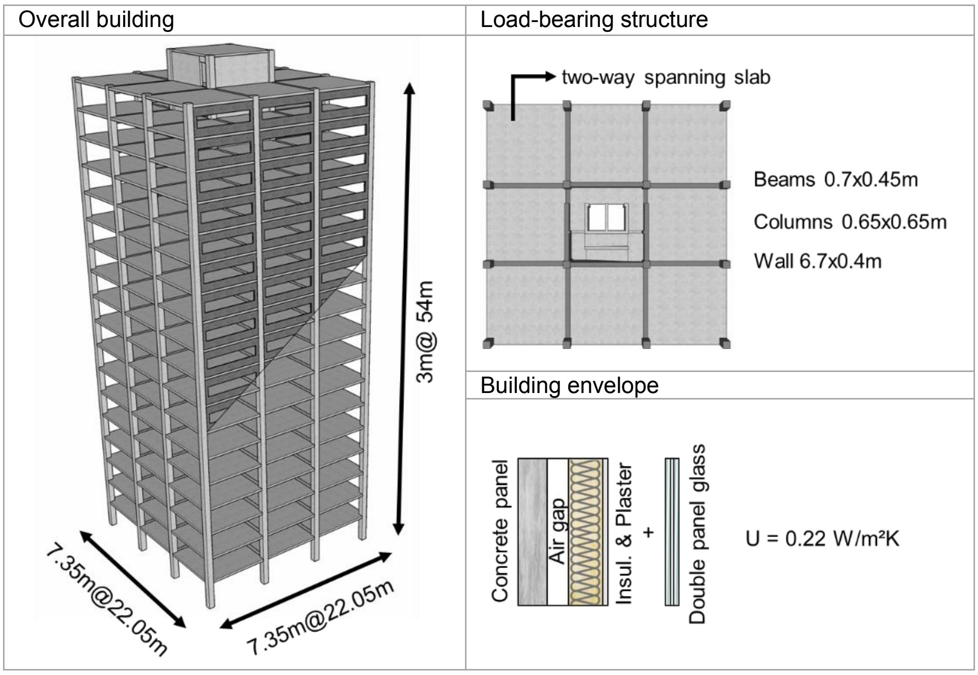

Figure 2: Case-study dimensions and properties.

The lateral loads resisting elements are the two internal frame-wall (dual) systems in each structural direction. A 2-way spanning flat slab 0.25m thick is responsible for ensuring the floor diaphragm, thus is properly connected to transfer the entire floor forces to the seismic-resistant systems. The building seismic mass is 736.0 tons per each floor, while the roof has a mass of 719.8 tons. The building façade is a modular prefabricated steel-stud panel systems with external insulated precast cladding panels and double pane windows, representing a new façade design (thermal transmittance of 0.22 W/m^{2}K, in order to satisfy the national guidelines for energy efficiency of building envelopes). Furthermore, all the other architectural components (drywall gypsum partitions, suspended ceilings), equipment (ideal HVAC systems) and contents (desktops, modular office tables, etc.) are identified and included in the loss modelling.

The study is implemented by considering two different locations in Europe: Messina (IT) and Bucharest (RO) both representing high-seismic prone areas. The cities are instead characterized by different climatic conditions: 1) Messina has a warm temperate Mediterranean climate with dry, warm summers and moderate, wet winters (Köppen-Geiger Climate Classification: "Csa": Mediterranean Climate); 2) Bucharest has a continental climate with cold winters and hot summers (Köppen-Geiger Climate Classification: "Cfa" - Humid Subtropical).

Both locations experienced multiple heatwaves in the past two decades (Figure 3). The most intense heatwave that struck the region of Bucharest took place in 2007 and lasted approximately 11 days, while for the region of Messina the most intense heatwave took place in 2021 and lasted for 60 days, the longest duration ever recorded [18]. The study uses these two periods to represent heat stress conditions. The weather data necessary to create a file in the EPW format, for use in the energy simulation, were sourced from the NOAA[1] and Copernicus online services [19]. Beside these historical data, the study considers the representative climate files (EPW IWEC data) for the two locations when designing the HVAC systems of the case study building.

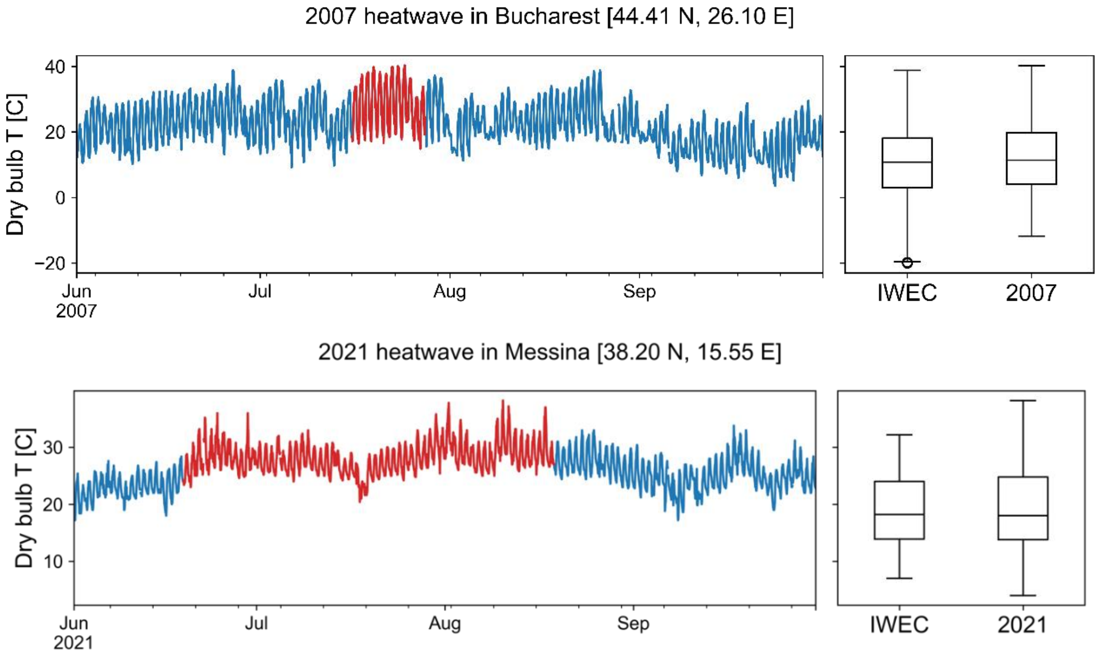

Figure 3: Dry bulb temperatures during the identified heatwaves event (left) and compared with typical temperatures used for building systems design and sizing (right).

3.1.1. Structural design

The structural/seismic design of the monolithic cast-in-situ building is implemented by referring to the above-mentioned building scheme, geometry and related vertical loads (self-weight, live loads) and following the principles of the Direct Displacement Based Design (DDBD) [20] adapted for frame-wall systems [21]. The structural/seismic design is carried out targeting a design drift limit (θ_d) that takes into account codes limitations, good practice and/or material strain limits, and assuming 40% as frame overturning-moment ratio (β_F), which represents the overturning moment contribution of the frame only system vs. the total (frame-wall) system. The design of the reinforced concrete high-rise building is implemented referring to the Maximum Credible Earthquake scenario for both locations, corresponding to an event with 2500 years return period (T_R). The corner period (T_D) and the peak (plateau) displacement spectral ordinate (Δ_D) are computed using the formula provided by Faccioli *et al.* [22], thus are defined as a function of the Moment Magnitude M_w, the fault rapture distance r (Figure 4a) and the local soil factor C_s. A firm ground soil is assumed for both locations (meaning a $C_s = 1$) while M_w and r were defined based on the local scenario to define the elastic acceleration and displacement spectra presented in Figure 4b.

[1] NOAA Integrated Surface Database (ISD) was accessed on 06/03/2023 from https://registry.opendata.aws/noaa-isd

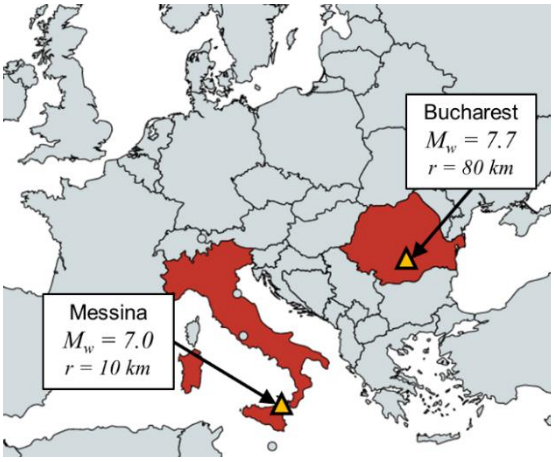

(a)

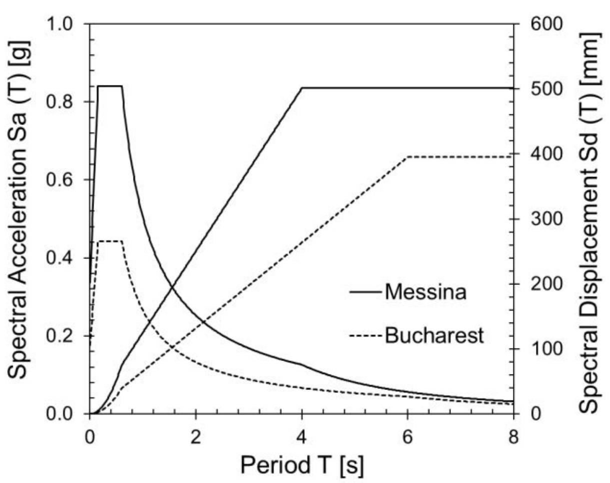

(b)

Figure 4: (a) Building locations and fault properties. (b) Elastic spectra derived from Faccioli et al. [22]

The response spectra are used to develop the DDBD procedure for designing the building in both seismic scenarios. Table 1 summarizes the main design parameters obtained from implementing the displacement-based design. By distributing the base shear from the DDBD throughout the overall structural system, the monolithic cast-in-situ connections are designed, i.e. the steel reinforcement (number and diameter of rebars) of the structural members are identified and, consequently, the local non-linear structural behavior in terms of Moment-Curvature at the end section of beams, columns and at the wall base.

Parameter	Messina	Bucharest
Effective Height, H_e [m]	39.1	40.3
Design Displacement, Δ_d [mm]	443.2	316.2
Effective Mass, m_e [t]	8879.0	8151.6
System Ductility, μ_{sys} [-]	2.5	1.3
Effective period, T_e [s]	4.3	5.6
Effective stiffness, K_e [kN/m]	19406.4	10119.2
Total Overturning Moment, OTM_{tot} [kNm]	168280.5	64435.1
Total Base Shear, $V_{b,tot}$ [kN]	4300.8	3200.0

Table 1: DDBD parameters for the Frame-Wall system.

3.2 Seismic modelling and analysis

Numerical modelling of both buildings is implemented in Ruaumoko2D software [23] following a lumped plasticity approach for the simulation of the local regions where the inelastic behavior is expected. The structural elements are therefore modelled as elastic members linked together through springs (simulating the plastic hinge regions), described by moment-rotation relationships and Takeda hysteresis rules. Façade systems are not modelled in this investigation, assuming a poor interaction with the main structure.

The numerical models are initially validated by performing non-linear static analyses: adaptive push-over and cyclic adaptive push-over to better describe the change of structural stiffness. In fact, the load lateral pattern changes every step depending on mass, new effective frequency and displacement shape. The push-over results (Figure 5a) provide useful indications on the expected capacity of both buildings before developing dynamic analyses, e.g. in terms of strength/stiffness values and sequence of plastic hinges forming during the analysis. For each site seven spectrum-compatible accelerograms are then selected from the European Strong Motion database using REXEL.DISP software [24]. A comparison between the Average Spectra and Design spectra is showed in Figure 5b, where it can be observed a maximum spectral difference of 20% until the corner periods. These records are finally considered for the numerical investigation.

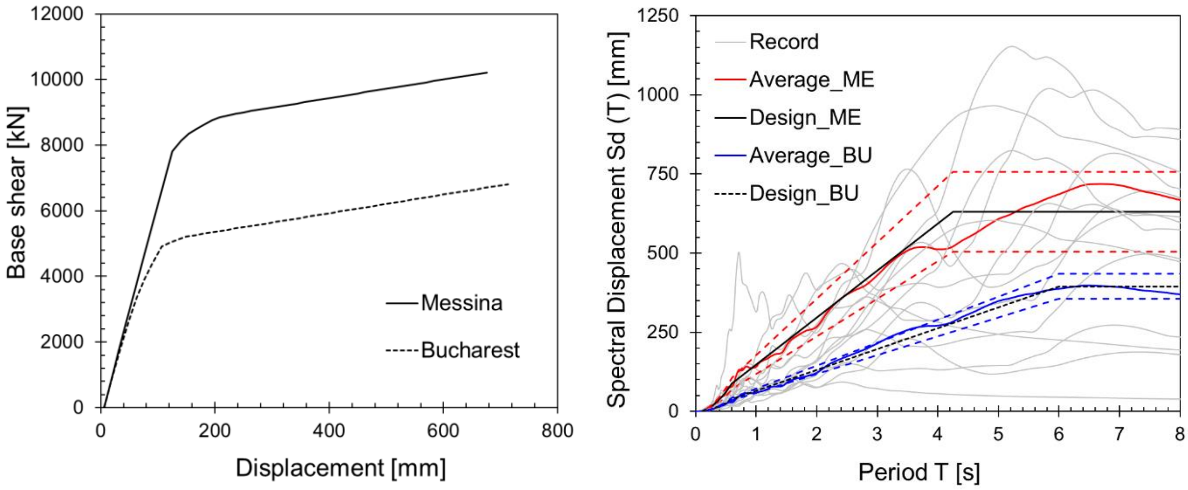

(a) (b)

Figure 5: (a) Capacity curves from adaptive push-over analysis; (b) Selected ground motions with average spectra for both cities of Messina (ME) and Bucharest (BU).

Non-linear time-history analyses are finally carried out to determine the seismic demand in terms of floor accelerations, inter-story drift ratios and residual displacements (Figure 6).

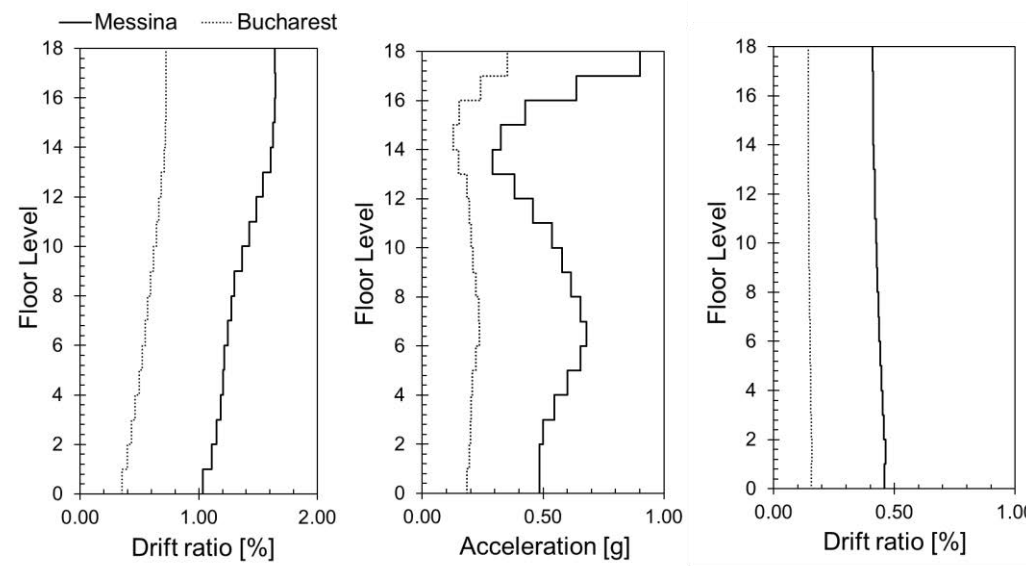

Figure 6: Inter-storey drift ratio, peak floor accelerations and residual drift ratios from time-history analyses.

It can be observed that higher demand parameters are recorded for the case study in Messina, as expected due to the implemented structural design targeting higher design displacement levels and higher earthquake intensities. For both buildings, an increase of floor accelerations is observed at the upper stories due to higher mode effects. The growing demand for faster acceleration in structures may result in increased damage to acceleration-sensitive components. The post-earthquake residual drift ratios are also recorded (less than 0.5%), being a critical damage indicator that can lead to partial or total loss of structural safety after earthquakes and therefore causing significant losses for a building.

To compute the expected losses, an intensity-based loss analysis is developed following the probabilistic methodology proposed in FEMA P-58 [7]. Input data for the loss assessment are the predicted accelerations and drift ratios as well as the fragility functions, thus the potential damage states, of all structural and non-structural building elements. Fragility and consequence data (as the repair costs) for monolithic cast-in-situ structural members, building facades and other components are defined from the FEMA P-58 fragility database. Moreover, the total building replacement costs are estimated accounting for the specific labor cost and including the quantities of concrete and steel rebars, the cost of formworks, safety, excavation, foundations and geotechnical surveys. Loss assessment results in terms of direct losses are finally elaborated to determine the probable maximum losses. In Figure 7a, the repair costs are shown as a loss curve. The results indicate that Messina and Bucharest experienced repair costs of 0.85% and 0.16%, respectively, as a ratio of the total building replacement cost. Notably, structural components accounted for the majority of the repair costs. As discussed earlier, the higher acceleration demand in Messina resulted in increased damage to acceleration-sensitive components on the upper floors, as depicted in Figure 7b.

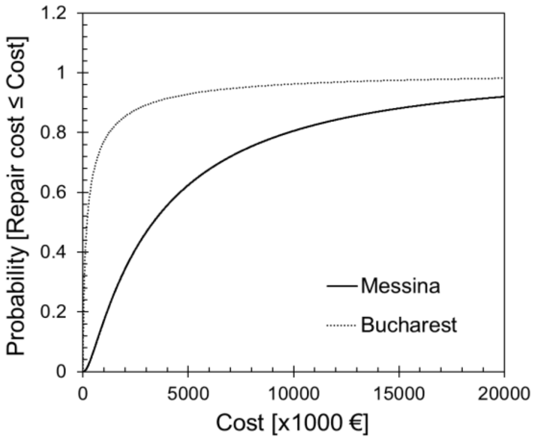

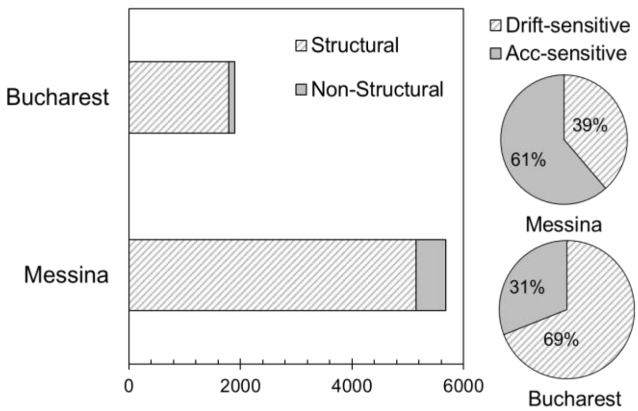

Figure 7: (a) Loss curves and (b) distribution of losses at building level.

The casualty results reveal a small percentage of injuries and fatalities, considering a building population of 160 people at time the earthquake occurred. Both buildings suffer the same collapse mode, which affect the second story thus resulting in the same number of losses. It is important to note that in this study, collapse modes are assumed to have an equal probability of occurring, and that the collapse of one level do not have a cascading effect on the levels below.

Expected Losses	Messina	Bucharest
Repair cost [x1000 €]	17,075	3,310
Injuries	0.48	0.48
Fatalities	4.35	4.35

Table 2: Maximum direct losses.

3.3 Energy and thermal analysis

The building model for the energy analysis is created in EnergyPlus software v. 9.1.0 [25] by modelling the thermal properties of the building as described in section 3.1. using a combination of geometry, material properties, and system specifications. To accurately represent the building physical and thermal properties, walls (Window-to-Wall ratio of 0.4), roofs, floors, windows (double pane) and doors are properly simulated in the model. Specifically, thermal conductivity, specific heat, density, and emissivity are assigned to each building element. The building model is then divided into thermal zones based on the occupancy and thermal characteristics. The zoning is indeed critical for capturing the dynamic interactions between different building elements and the HVAC system.

Design requirements are set for the internal comfort of building occupants. The cooling set point temperature is 24 °C and the heating set point temperature is 19 °C. For the internal heat gain of either office or residential floors, equipment load is 5 or 10 W/m2 , artificial lighting load is 10 or 5 W/m2 , while the density of occupation is 0.01 or 0.005 persons per square meter. The desired rate of outside air infiltration is 0.0003 m3 /s per square meter of floor. The HVAC is modelled as an Ideal Load System, where therefore inefficiencies of the system are not taken into account. The maximum cooling capacity is determined by first calculating the cooling demand during the design day found in ddy file for each location (Bucharest and Messina). Once the cooling capacity is defined for each zone, the thermal simulation is again run to calculate the indoor operative temperature in each zone. These values are then used to calculate the cumulative number of hours above the comfort thresholds.

The heat wave related social losses are computed by calculating the cumulative number of hours that are above the comfort threshold. In addition, the economic losses are computed by considering the increased in total energy consumption due to the heat wave. Figure 8 shows the total cumulative hours when the operative temperature is above the thresholds of 26 °C, 28 °C, 30 °C and 32 °C. The heatwave in Messina is characterized by higher extreme temperatures and longer times which determine a larger number of hours in extreme discomfort, especially above the threshold of 28 °C. The number of hours in extreme discomfort (above 32 °C), it is instead comparable despite the heatwave in Messina being much longer. The increase in energy consumption due to the heatwave is larger in Messina, which is characterized by more extreme temperatures and larger cooling capacity, while the overall energy consumption is larger in Bucharest since it is driven by the heating season (Figure 9), but proportionally the increase in energy demand is higher for Bucharest than for Messina. This is also a limitation of sizing the cooling capacity based on the design days rather than on actual historical weather.

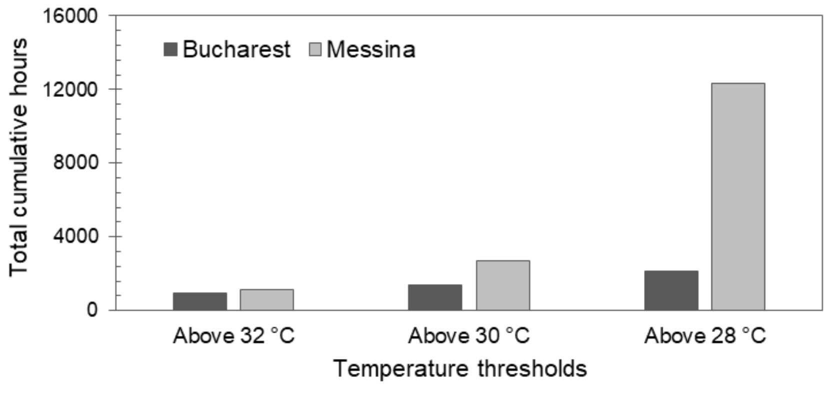

Figure 8: Total cumulative number of hours above 32, 30 and 28 °C.

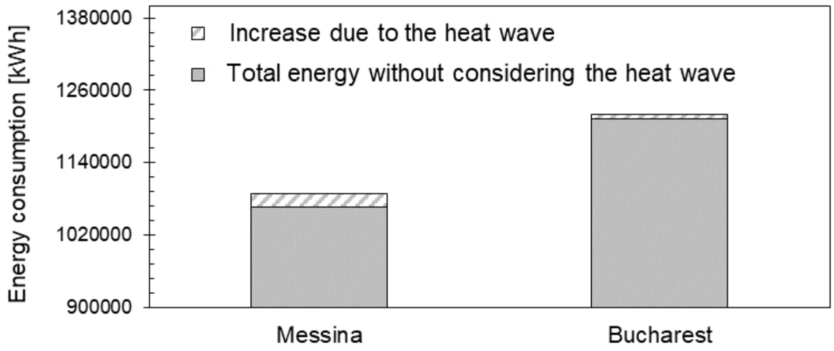

Figure 9: Total energy consumption due to heat wave

Table 3 summarizes the total losses due to heatwave for both Bucharest and Messina, and the related economic losses/cost (considering 0.43 and 0.16 € per kWh of electricity for Messina and Bucharest respectively). Given that in Romania the cost of the energy is lower, the impact of the heatwave is lower than in Italy in terms of energy cost.

Expected Losses	Messina	Bucharest
Total cumulative hours of extreme discomfort (T>28 °C)	2690	2143
Total cumulative hours of extreme discomfort (T> 32 °C)	1138	935
Total annual energy consumption [kWh/m^2]	123.58	139.73
Total annual energy consumption including the heat wave [kWh/m^2]	125.3	141.36
Total energy consumption [kWh]	1,066,835	1,213,376
Total energy consumption including the heat wave [kWh]	1,088,623	1,220,332
Total increase in energy due to the heat wave [kWh]	21,788	6,956
Total increase in energy per m^2 [kWh/m^2]	1.72	1.63
Total increase in energy cost [€]	9,370	1051
Increased energy cost per m^2 [€/m^2]	0.74	0.26

Table 3: Maximum direct losses due to heat wave hazards.

3.4 Earthquakes vs. heat waves impact

Results from the seismic and energy simulations are finally compared to assess the socio-economic impact of the different hazards. The comparison is shown in Figure 10a in terms of overall decision variables including the repair cost and the number of injuries/fatalities for earthquakes, as well as the annual energy cost and the discomfort hours for the heat wave scenario. The graph demonstrates that the Messina case study was more significantly affected by the hazards examined, with the exception of seismic casualties. This is due to the modeling assumptions that resulted in a realization with the same failure mode for both case studies, leading to the same number of casualties in buildings with the same population. The difference between the two case studies is further shown in Figure 10b, where the same scaling in terms of percentage value is adopted for comparing the results. Specifically, the economic losses are expressed as percentage of the total building cost (replacement cost in case of earthquake, thus including the demolition cost). The social impact is instead assessed focusing on the severe danger condition, meaning number of deaths as a percentage of the total building population for the earthquake vs. the number of discomfort hours (temperature higher than 32 °C) as percentage of the total hours in a year for the heat wave. As expected, the comparison reveals that earthquakes have a significant impact on direct economic losses, whereas heat waves are more likely to cause extreme discomfort, potentially resulting in mortality.

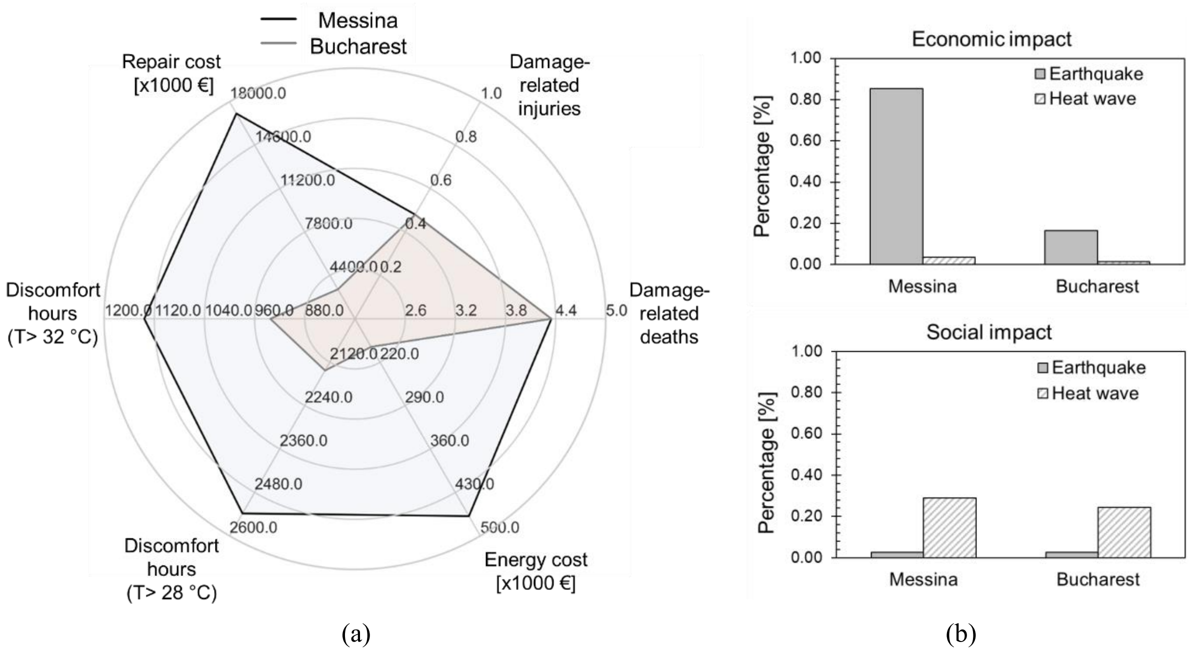

Figure 10: (a) Comparison in terms of decision variables. (b) Economic and social impact of earthquake vs. heat wave scenarios.

4 CONCLUSIONS

The paper discusses the impact of earthquakes and climate change-induced heat waves on buildings in terms of socio-economic impact, thus emphasizing the need for increased resilience and multi-risk analysis. The study is implemented for a high-rise building by means of numerical modelling in order to estimate repair costs, injuries/fatalities in case of earthquake, as well as weather-related power consumption and discomfort hours in case of extreme heat events. The study is implemented for two different locations in Europe (Messina, Bucharest) with high seismicity (but different magnitude and fault distance) and different climatic conditions (warm temperate vs. continental climate). The heat waves scenarios are obtained from historical data considering the most extreme event recorded in the last years. The results of seismic and energy dynamic simulations are finally compared to assess the impact of the two hazards on building performance and potential consequences. It is found that the case study in Messina is affected by higher seismic and energy economic losses, although the energy consumptions are higher in Bucharest where the energy cost has a lower price. The investigation also revealed that Messina experiences a greater number of hours in extreme discomfort, attributable to its higher temperatures and longer duration of high temperatures. Despite this, the implemented seismic loss modelling assumptions yielded the same expected number of casualties for both buildings, due to one probabilistic-based realization experiencing the same collapse mode. Overall, the study highlights the greater economic losses associated with earthquakes, while also underscoring the potential for heat waves to cause fatalities, given their increasing frequency and severity.

However, the study has some limitations that need to be addressed in future research. Firstly, the collapse modes and their cascading consequences at the building level should be properly investigated to quantify the potential damage area and resulting casualties. The sequence of mechanisms occurring and their correlation at the building level should be taken into consideration and implemented in the study. Furthermore, the study should account for different earthquake scenarios (ranging from low-to-high) with varying return periods. The cooling capacity of a building is a crucial factor in determining its preparedness to withstand heat waves and the associated economic losses. Design days and weather predictions are important considerations that can inform cooling requirements. Metrics used to assess thermal discomfort and the impact of heat waves on human health can affect the overall risk of a building. While the cooling capacity of an existing building is usually known, further work is needed to define the most accurate procedure for evaluating the cooling capacity of new buildings. Additionally, additional research is needed to identify the best metrics to predict the risk of human discomfort and health due to extreme temperatures caused by heat waves.

This investigation underscores the need for further research and the development of methods that can effectively evaluate the cumulative impact of earthquakes and heat waves on buildings and infrastructure. To assess the cumulative losses, an integrated approach should be adopted that considers the probability of both events occurring within a life-cycle framework. This requires the development of new assessment methodologies that take into account the potential interdependence and cascading effects between earthquakes and heat waves. Such methodologies would enable better decision-making by policymakers, building designers, and engineers to develop more resilient buildings and infrastructure that can withstand multiple hazards.

5 REFERENCES

[1] EEA, *Economic losses from climate-related extremes in Europe*. European Environmental Agency, Copenhagen, Denmark, 2019.

[2] L. Dal Zilio, J.P. Ampuero, Earthquake doublet in Turkey and Syria. *Communications Earth & Environment*, **4**, 71, 2023.

[3] FEMA, *HAZUS-MH MR3 Technical Manual*. Federal Emergency Management Agency, Washington, USA, 2003.

[4] H. Crowley, J. Dabbeek, V. Despotaki, D. Rodrigues, L. Martins, V. Silva, X. Romão, N. Pereira, G. Weatherill, L. Danciu, *European Seismic Risk Model (ESRM20)*. EFEHR Technical Report 002 V1.0.0, 2021.

[5] J. Moehle, G. Deierlein, A framework methodology for performance-based earthquake engineering. *13th World Conference on Earthquake Engineering (13WCEE)*, Vancouver, B.C., Canada, August 1-6, 2003.

[6] K.A. Porter, An Overview of PEER's Performance-Based Earthquake Engineering Methodology. *9th International Conference on Applications of Statistics and Probability in Civil Engineering (ICASP9)*, San Francisco, California, United States, July 6-9, 2003.

[7] FEMA, *Seismic Performance Assessment of Buildings, Volume 1 – Methodology*. Technical Report FEMA-P-58-1, Federal Emergency Management Agency, Washington, United States, 2012.

[8] D. Cardone, A. Flora, M. De Luca Picione, A. Martoccia, Estimating direct and indirect losses due to earthquake damage in residential RC buildings. *Soil Dynamics and Earthquake Engineering*, **126**, 2019.

[9] F.A. Arifin, T.J. Sullivan, G. MacRae, M. Kurata, T. Takeda, Lessons for loss assessment from the Canterbury earthquakes: a 22-storey building. *Bulletin of Earthquake Engineering,* **19**, 2081–2104, 2021.

[10] S. Bianchi, J. Ciurlanti, S. Pampanin, Comparison of traditional vs. low-damage structural & non-structural building systems through a cost/performance-based evaluation. *Earthquake Spectra*, 1-20.

[11] S. Homaei, M. Hamdy, Thermal resilient buildings: How to be quantified? A novel benchmarking framework and labelling metric. *Building and Environment*, **201**, 2021.

[12] A. Sakka, M. Santamourisa, I. Livadaa, F. Nicolb, M. Wilson, On the thermal performance of low income housing during heat waves. *Energy and Buildings*, **49**, 2012.

[13] S. Bucking, M. Rostami, J. Reinhart, M. St-Jacques, On modelling of resiliency events using building performance simulation: a multi-objective approach. *Journal of Building Performance Simulation*, **15**, 3, 307-322, 2022.

[14] C.Y. Siu, W. O'Brien, M. Touchie, M. Armstrong, A. Laouadi, A. Gaur, Z. Jandaghian, I. Macdonald, Evaluating thermal resilience of building designs using building performance simulation–A review of existing practices. *Building and Environment*, 2023.

[15] S. Tong, X. Wang, W. Yu, D. Chen, X. Wang, The impact of heatwaves on mortality in Australia: A multicity study, *BMJ Open*, **4**, 2, 2014.

[16] M. Alam, J. Sanjayan, P. X. W. Zou, M. G. Stewart, J. Wilson, Modelling the correlation between building energy ratings and heat-related mortality and morbidity. *Sustainable cities and society*, **22**, 29-39, 2022.

[17] J. Ciurlanti, S. Bianchi, S. Pampanin, Feasibility Study of Low-Damage Technology for High-Rise Precast Concrete Buildings. *SECED 2019 Conference*, London, England, 2019.

[18] O. Lhotka, J. Kyselý, The 2021 European Heat Wave in the Context of Past Major Heat Waves. *Earth and Space Science*, **9**, 11, 2022.

[19] M. Schroedter-Homscheidt, F. Azam, J. Betcke, N. Hanrieder, M. Lefèvre, L. Saboret, Y.-M Saint-Drenan. Surface solar irradiation retrieval from MSG/SEVIRI based on APOLLO Next Generation and HELIOSAT-4 methods, *Contrib. Atm. Sci./Meteorol. Z.*, 2022.

[20] M. J. N. Priestley, G. M. Calvi, M. J. Kowalsky, *Direct Displacement-Based Seismic Design of Structures*, IUSS Press, Pavia, Italy, 2007.

[21] A. R. R. Abellán, T. J. Sullivan, S. Pampanin, Adapting DDBD for the design of Frame-Wall Structures with Hybrid-Rocking Joints, *15th World Conference of Earthquake Engineering*, Lisbon, Portugal, 2012.

[22] E. Faccioli, R. Paolucci, J. Rey, Displacement spectra for long periods, *Earthquake Spectra*, **20**, 2, 347-376, 2004.

[23] A.J. Carr, *Ruaumoko Program for Inelastic Dynamic Analysis – User Manual*, University of Canterbury, Christchurch, New Zealand, 2003.

[24] C. Smerzini, C. Galasso, I. Iervolino, R. Paolucci, Ground motion record selection based on broadband spectral compatibility, *Earthquake Spectra*, **30**, 4, 1427–1448, 2013.

US Department of Energy's Building Technologies Office. *EnergyPlus*. DOE-BTO, 2001.